



Spectral Graph Clustering for Intentional Islanding Operations in Resilient Hybrid Energy Systems

Jiaxin Wu, Xin Chen, Sobhan Badakhshan, *Graduate Student Member, IEEE*,
Jie Zhang , *Senior Member, IEEE*, and Pingfeng Wang , *Member, IEEE*

I. INTRODUCTION

Abstract—Establishing cleaner energy generation, therefore, improving the sustainability of the power system is a crucial task in this century, and one of the key strategies being pursued is to shift the dependence on fossil fuel to renewable technologies, such as wind, solar, and nuclear. However, with the increasing number of heterogeneous components included, the complexity of the hybrid energy system becomes more significant, and the complex system imposes a more stringent requirement of the contingency plan to enhance the overall system resilience. Among different strategies to ensure a reliable system, intentional islanding is commonly applied in practical applications for power systems and attracts abundant interest in the literature. In this study, we propose a hierarchical spectral clustering-based intentional islanding strategy at the transmission level with renewable generations. To incorporate the renewable generation that relies on the inverter technology, the frequency measurements are considered to represent the transient response, and it has been further used as embedded information in the clustering algorithm along with other important electrical information from the system to enrich the modeling capability of the proposed framework. To demonstrate the effectiveness of the islanding strategy, the modified IEEE 9-bus system coupled with wind farms is considered as the test case.

Index Terms—Disruption management, intentional islanding, renewable, resilience.

WITH the increases on both scale and complexity, hybrid energy systems (HESs) consisting of various types of generation technologies, become more vulnerable toward disruptive events. Such vulnerability, therefore, drives the research efforts leading to robust HESs. Also, for large-scale HESs, mitigating the cascading effects after the occurrences of disruptive events is a crucial task for attaining reliable system operations. To comprehend the system's capability toward uncertain disruptive scenarios, researchers have adopted the term “resilience” from the ecology field. Different from the terminology of system reliability, in which the degraded system performance and the possibility of failure are studied, the resilience metric is utilized to complement the analysis of real-time system behavior. A resilient system should not only proactively withstand impacts of disruptive events but also need to acquire the capability of self-healing from damages.

Motivated by the requirement for a resilient system, different frameworks have been proposed to help the HES establish self-healing capability. Here, we categorize the research efforts about resilience in terms of the temporal stages of the proposed frameworks, i.e., before and after the disruptions, as shown in Fig. 1. During the steady state, first it is important to obtain a universal analytic framework to assess the system resilience level [1]. It is also beneficial to optimize the system resilience during the design stage by conducting proactive system health management [2]. Although comprehensive predisruption frameworks have been proposed, how a system should behave after disruptions thus to preserve resilient performance is still unknown, and without an appropriate postdisruption guiding/response framework, cascading failures induced by severe disruptions are inevitable, especially in closely coupled network systems. As a result, it is required to study suitable recovery strategies to ensure system resilience.

To achieve the self-healing capability of the system, several real-time operational frameworks have been proposed to guide how the system should behave after disturbances. For instance, researchers try to attain a resilient operational framework by incorporating optimal scheduling for repair resources with uncertainties [3], forming self-sustainable subsystems [4], and guided recovery through control strategies [5]. Those studies focus on solving for the optimal decisions of how to utilize the

Manuscript received 16 March 2022; revised 7 July 2022; accepted 10 August 2022. Date of publication 17 August 2022; date of current version 22 March 2023. This research was supported in part by the National Science Foundation through the Engineering Research Center for Power Optimization of Electro-Thermal Systems (POETS) with cooperative agreement EEC-1449548, and in part by the U.S. Department of Energy's Office of Nuclear Energy under Award No. DE-NE0008899. Paper no. TII-22-1093. (Corresponding author: Pingfeng Wang.)

Jiaxin Wu, Xin Chen, and Pingfeng Wang are with the Department of Industrial and Enterprise Systems Engineering, University of Illinois Urbana-Champaign, Urbana, IL 61801 USA (e-mail: jiaxinw3@illinois.edu; xinchen@illinois.edu; pingfeng@illinois.edu).

Sobhan Badakhshan and Jie Zhang are with the Department of Mechanical Engineering and (Affiliated) the Department of Electrical and Computer Engineering, University of Texas at Dallas, Richardson, TX 75080 USA (e-mail: sobhan.badakhshan@utdallas.edu; jiezhang@utdallas.edu).

Color versions of one or more figures in this article are available at <https://doi.org/10.1109/TII.2022.3199240>.

Digital Object Identifier 10.1109/TII.2022.3199240

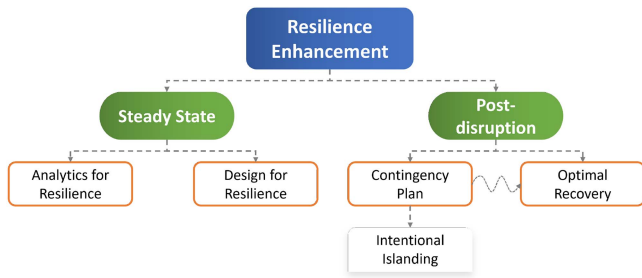


Fig. 1. Studies for resilience enhancement can be categorized into two groups, while the intentional islanding is one of the contingency plans after disruptions.

backup resources to recover the HES, on the basis of having a contingency plan, such as the network reconfiguration beforehand. That is, during the postdisruption stage, the self-recovery capability is realized in two steps: an appropriate emergency response, e.g., system reconfiguration, followed by performing optimal restorations. As a result of the necessary sequential order, setting up a reliable system reconfiguration plan before conducting optimal recovery is vital for ensuring the system resilience, and in the power system field, the system reconfiguration is widely used as a contingency plan for a robust system [6], [7], [8].

The main objective of reconfiguration/islanding is to derive the optimal plan for allocating buses of the HES into appropriate disconnected subsystems. Thus, the system can isolate failures and sustain nominal performance with the presence of disruptions. Such a contingency plan coincides with the goal of clustering algorithms. Therefore, proposed intentional islanding strategies usually use the graph clustering method as the building block. For example, Esmaeilian et al. [9] proposed a spectral clustering-based intentional islanding strategy to regulate the systems after disruptions, considering solely the system power flow as the major performance criterion. Moreover, to mitigate the effect of the presumption on the number of islands after disruptions, Sanchez-Garcia et al. [10] utilized the unsupervised hierarchical clustering technique to conduct the system partitioning. Saadipour-Hanzaie et al. [11] introduced a coherency identification method to achieve robust islanding operations based on online frequency measurement data. Dabbaghjamanesh et al. [12] improved the robustness of the intentional islanding strategy by considering multiple electrical information embedded in the system along with the dynamic power flow measurement in the algorithm.

However, existing intentional islanding strategies usually utilize limited system information to derive the clustering results, for example, the generator coherency identified by frequency deviations or rotor angles. With more advanced power monitoring unit technologies, it is required to investigate data-driven methods that can fully utilize various power system measurement data. Besides, most of the proposed frameworks only provide deterministic islanding solutions. But with the increasing system complexity, the online measurement information can vary along the way [13] and uncertainties during operations are hard to avoid: islanding solutions with more flexibility become

desirable. In addition, traditional methods are focusing on power systems only with synchronous generators and usually rely on a specific set of system measurements or generator coherency. As for modern power grids with a high level of renewable penetrations, the system performance will be largely influenced by the behavior of the inverter-based generation. Hence, how to perform the intentional islanding operation for power systems with renewable penetration is still a crucial challenge.

In this article, we demonstrate a new intentional islanding method based on the clustering algorithm for HES with various levels of renewable penetrations to enable the self-recovery capability. Our proposed framework utilizes the hierarchical spectral clustering technique based on both systems' static and dynamic information, and the advantages can be concluded in three folds as follows.

- 1) The spectral clustering method is coupled with the Grassmann manifold so that the islanding decision can rely on system online information collected from different channels: the Grassmann manifold unifies heterogeneous measurement data into one single source, which can be directly used as the input to the clustering algorithm.
- 2) The hierarchical clustering is used to output the islanding result: rather than generating a deterministic solution, it provides the decision maker with comprehensive clustering results that have different granularity. This characteristic leads to versatile islanding choices that decision makers can adapt to different online conditions.
- 3) To work for modern systems with a high-level penetration of renewable generations, the frequency deviation signal at the point of common coupling (PCC) is employed in the Grassmann manifold: this extra signal helps determine the coherency between the renewable generations and the rest of the grid.

The rest of this article is organized as follows. Section II introduces the proposed intentional islanding methodology in detail, where the spectral graph clustering algorithm is coupled with the Grassmann manifold technique to accommodate the heterogeneous information extracted from the system. Section III presents case study results based on the IEEE 9-bus test system to validate the proposed islanding framework. Finally, Section IV summarizes the study along with discussion about future research directions.

II. CLUSTERING FOR INTENTIONAL ISLANDING

The intentional islanding is usually realized by conducting node clustering for the power system represented as a graph. As for the clustering methods, the k-means algorithm is widely used for identifying the inherent patterns of high-dimensional data. The algorithm assumes that each sample point belongs exclusively to one group, and it assigns the data point X_j to the cluster S_i in terms of minimizing the overall Euclidean distance from the cluster center μ_i to each point, and the overall objective for a dataset with n samples can be expressed as follows:

$$\arg \min_S \sum_{j=1}^n \sum_{X_j \in S_i} \|X_j - \mu_i\|^2. \quad (1)$$

Although the k-means algorithm has adequate clustering performance for tabular data, it cannot be directly applied to graph-structured data obtained from HESs. Since the Euclidean distance cannot directly reflect the difference between the nodes in the grid. To remedy this limitation of the k-means algorithm, spectral graph theory can be incorporated. To be self-contained, we introduce the spectral clustering algorithm as well as the mechanism for embedding the graphical information in the following sections.

A. Spectral Graph Theory

Let a graph $\mathcal{G} = (\mathcal{V}, \mathcal{E})$ with vertex set \mathcal{V} and edge set \mathcal{E} represent the interconnected system. To be specific, for a N -bus power system, the corresponding graphical notation can be written as $\mathcal{V} := \{1, 2, \dots, N\}$ and $\mathcal{E} := V \times V$. In the graph, the buses carrying loads/generations are the vertices while the transmission lines are the edges. Moreover, based on the connection status between each pair of buses, a square connectivity matrix $W_{ij}^t \in \mathbb{R}^{V \times V}$ can be constructed as follows:

$$W_{ij}^t = \begin{cases} 1 & \text{if } (i, j) \in \mathcal{E} \\ 0 & \text{otherwise.} \end{cases} \quad (2)$$

The W_{ij}^t is symmetric and follows the convention that all diagonal entries equal to zero, i.e., no self-loop. The connectivity matrix solely indicates the geological connectivity of the grid. Besides the connectivity matrix, the power system requires other matrices to embed the electrical information it preserves, such as the power flow and resistance/reactance. Thus, by using W_{ij}^t as an analogy, matrices for the electrical properties are defined as follows:

$$W_{ij}^p = \begin{cases} \frac{|P_{ij}| + |P_{ji}|}{2} & \text{if } (i, j) \in \mathcal{E} \\ 0 & \text{otherwise} \end{cases} \quad (3)$$

where P_{ij} and P_{ji} are the active power flow on each transmission line considering the line loss, and the matrix for admittance of the system can be obtained as follows:

$$W_{ij}^a = \begin{cases} \frac{1}{\sqrt{R_{ij}^2 + X_{ij}^2}} & \text{if } (i, j) \in \mathcal{E} \\ 0 & \text{otherwise} \end{cases} \quad (4)$$

where R_{ij} and X_{ij} are the resistance and reactance of the transmission lines, respectively. Similar to the connectivity matrix W_{ij}^t , the power flow matrix W_{ij}^p and admittance matrix W_{ij}^a are also symmetric with all diagonal entries being zeros.

The entries of aforementioned three weight matrices measure how strong a line connection would be when partitioning nodes. In other words, disconnecting a transmission line with a large weight to form islands will lead to a large penalty in the objective of the clustering algorithm, and this behavior is desirable for intentional islanding in power grids. Since buses directly connected are more likely to stay in the same cluster with similar operating conditions. Moreover, in W_{ij}^a , a larger entry means a shorter electrical distance, and the buses connected by a transmission line with a small electrical distance should be in the same cluster after the islanding. Similarly, a pair of nodes in W_{ij}^p carrying large power flow should not be cut and form isolated

islands, which could lead to a large imbalance in load/generation and load shedding. Notice that the electrical information used in the intentional islanding algorithm are not limited to the aforementioned three matrices. Based on the prior knowledge of the decision maker, other important online measurements from the HES can also be used to represent the system status and thus treated as the matrical inputs of the algorithm.

In order to cluster nodes based on introduced weight matrices and fulfill the intentional islanding task, we need to further derive the Laplacian matrix of the graph. The Laplacian matrix embeds the nodal information from the graph system into a pseudotabular form, which can be directly used as the inputs of clustering algorithms, and it is defined as $L = D - W$ where D is the degree matrix of the graph, which is a diagonal matrix obtained from $D = \text{diag}(\sum_j W_{ij})$. That is, the degree matrix D has all zeros on its nondiagonal entries, while the diagonal elements are the row sum of the weight matrix. In this way, each element of the Laplacian matrix has the form

$$L_{ij} = \begin{cases} d_i & \text{if } i = j \\ -w_{ij} & \text{if } (i, j) \in \mathcal{E} \\ 0 & \text{otherwise} \end{cases} \quad (5)$$

where d_i is the degree of node i . Usually, we will work on the normalized Laplacian matrix, which is scale independent and has better results for clustering. The normalized Laplacian matrix is calculated as $L_n = D^{1/2} L D^{-1/2}$. After normalization, the entries of the Laplacian matrix are

$$[L_n]_{ij} = \begin{cases} 1 & \text{if } i = j \\ \frac{-w_{ij}}{\sqrt{d_i d_j}} & \text{if } (i, j) \in \mathcal{E} \\ 0 & \text{otherwise.} \end{cases} \quad (6)$$

One characteristic of the Laplacian matrix is that it has the spectral information of the graph. We can perform eigendecomposition on the Laplacian matrix and treat the eigenvectors as the spectral embeddings. Then, by conducting clustering on these obtained spectral embeddings, we can discover the latent clusters for the network system. The overall roadmap of such a clustering technique is to use the first K eigenvectors of the Laplacian matrix as the geometric coordinates of the N data points defined in \mathbb{R}^K . Then these coordinates can be treated as in Euclidean space and be clustered by standard clustering techniques, such as the k-means algorithm. Notice that all spectra of the normalized graph Laplacian, i.e., its eigenvalues, always lie between zero and two. This magnitude is desirable when calculating the nodal similarities based on the corresponding eigenvectors.

B. Hierarchical Spectral Clustering

In Section II-A, we have briefly introduced the spectral clustering algorithm for graph systems based on the k-means algorithm. However, one drawback of the k-means-based spectral clustering is that the number of clusters, K , needs to be predefined. As for intentional islanding to avoid cascading failures, the number of islands cannot be easily assumed beforehand but need to be determined based on the online operational condition. To overcome this limitation of the k-means algorithm, this study

utilizes hierarchical clustering on the spectral domain of the graph.

Different from the k-means algorithm, which directly outputs results with a predefined number of clusters K and omits the inner connection between the nodes in the same cluster, the hierarchical clustering provides partitioning results with finer intracluster detail. The results of the hierarchical clustering are usually interpreted by the tree-like dendrogram, where each leaf is the individual node in the graph. The leaves of the dendrogram can also be viewed as clusters with a cardinality of one, and the goal of the clustering algorithm is to merge the closest clusters into a bigger cluster at each step following a bottom-up approach. To determine the best merging decision, the Wade linkage criterion [14] is used as the metric in this study

$$d(u, v) = \sqrt{\frac{|v| + |s|}{T} d(v, s)^2 + \frac{|v| + |t|}{T} d(v, t)^2 - \frac{|v|}{T} d(s, t)^2} \quad (7)$$

where u is a merged cluster from subclusters s and t , v is a unused cluster in parallel with s and t , $|\cdot|$ is the cardinality operator, and T equals the sum of $|s|$, $|t|$, and $|v|$. The Wade linkage criterion is a variance minimization metric and picks two clusters to form one that leads to the lowest sum of squared differences within the clusters. This variance minimizing characteristic makes the Wade linkage criterion similar to the objective of the traditional k-means algorithm, but in a hierarchical setting. Again, with the Wade linkage criterion, the goal is to merge two clusters with the smallest $d(u, v)$ until all nodes are merged into a single cluster, which is the root of the dendrogram.

After performing the hierarchical clustering, the dendrogram of the clustering results can be derived. Fig. 5 shows an example of the dendrograms from clustering nine nodes. As for an HES, after a disruptive event, the decision maker can determine the number of subsystems to form based on the specific system status, and the clustering results can be obtained by cutting the dendrogram at the corresponding level. For instance, if three clusters are preferred for the clustering results shown in Fig. 5, then the islanding results can be obtained by cutting the tree at a level around $d = 1.0$ to have three clusters $\{8, 2, 7\}$, $\{5, 1, 4\}$, and $\{6, 3, 9\}$. The advantage of obtaining the tree-like results for clustering is that it reveals a finer structure of the system, compared to directly outputting the partitions by using the traditional k-means algorithm. At various levels of the clustering resolution, the practitioner can zoom in or out to examine different structures of the clusters, and follow how each cluster is formed hierarchically.

C. Grassmann Manifold

Although the hierarchical clustering can expose a more detailed islanding results for HESs compared to the traditional k-means, the aforementioned algorithm has not considered the multiple Laplacian matrix defined simultaneously. In [10], the authors demonstrate different intentional islanding results by using Laplacian matrices derived from the average power flow and the admittance. But the scale of heterogeneous information embedded in the Laplacian matrix may be different, and it is required to normalize the magnitude to a unified range before

executing the clustering process. Thus, how to combine all different kinds of electrical information of the power system remains to be answered. Rather than treating different types of the Laplacian matrices separately, as in [10], here we adopt the Grassmann manifold for multiple matrices in order to derive a unified Laplacian matrix for clustering.

A Grassmann manifold $G(K, N)$ can be defined as the set of K -dimensional linear subspaces in \mathbb{R}^N , where each distinct subspace is mapped to an unique point on the manifold. Therefore, information embedded in different spaces can be mapped into an unified space and the clustering algorithm can utilize the mapped information to derive islanding results. We summarize the key steps from [15] for finding a unified Laplacian matrix of a graph with M distinct information matrices as follows.

- 1) Derive Laplacian matrix L_i for each graph G_i defined based on different weight matrices.
- 2) Each G_i can be approximated by the spectral embeddings matrix $U_i \in \mathbb{R}^{N \times K}$ from the first K eigenvectors of L_i .
- 3) Each U_i can be considered as a K -dimensional subspaces in \mathbb{R}^N .
- 4) The main objective becomes combing these several subspaces by finding a typical subspace $\text{span}(U)$, which is closest to all the subspaces $\text{span}(U_i)$; this can be written as a minimization program

$$\min_{U \in \mathbb{R}^{N \times K}} \sum_{i=1}^M \text{tr}(U^T L_i U) + \alpha \left[kM - \sum_{i=1}^M \text{tr}(U U^T U_i U_i^T) \right]. \quad (8)$$

- 5) The solution to the above minimization problem is the unified Laplacian matrix for clustering

$$L_{\text{uni}} = \sum_{i=1}^M L_i - \alpha \sum_{i=1}^M U_i U_i^T. \quad (9)$$

D. Choose the Embedding Space

Once a unified Laplacian matrix is derived from multiple Laplacian matrices, as shown in (9), then the intentional islanding can be achieved by performing hierarchical clustering on the Laplacian matrix as the global spectral embedding of the graph. Although we do not need to specify the number of clusters K beforehand to perform the hierarchical clustering, there is still a decision for choosing the subspace dimension K to embed the network system. Without explicit information about the generator coherency, the number of desired dimensions K is unknown and can be problem dependent. But one practical approach to make the optimal decision for the subspace dimension is to calculate the eigenvalues of the Laplacian matrix and treat the eigengap as a metric. The eigengap is the difference between the consecutive eigenvalues and can be found by

$$\gamma(\lambda_i) = |\lambda_{i+1} - \lambda_i| \quad (10)$$

where λ_i is the i th eigenvalue of the Laplacian matrix, and the normalized eigengap measured in percentage can be obtained

from

$$\gamma_n(\lambda_i) = \frac{\gamma(\lambda_i)}{\lambda_{i+1}}. \quad (11)$$

After deriving the eigengaps, how to determine the optimal K remains to be discussed. Here we need to introduce the basic metric used to measure the quality of the intentional islanding without the electrical properties. Let us denote the volume of a cluster as $\text{vol}(A) = \sum_{i \in A, j \in A} W_{ij}$, where A is a subset of the vertices that form the cluster. Based on the expression of the $\text{Vol}(A)$, one can see that it actually measures the closeness of the nodes inside the same cluster. Moreover, the boundary of the cluster is denoted as $b(A) = \sum_{i \in A, j \notin A} W_{ij}$, which measures the strength of interaction between the cluster and neighbors outside the cluster A , and the conductance $\Phi(A)$ of the cluster A is defined as the quotient $\frac{b(A)}{\text{vol}(A)}$. For an effective clustering strategy, the goal is to partition the graph into clusters with the smallest conductance. In other words, the optimal islanding results should only include clusters that have strong interactions within the cluster and weak connections to the rest of the graph outside the cluster. Formally, this clustering task can be written as the k -way partitioning problem [16]. Multiple subsets of vertices, i.e., clusters, A_1, \dots, A_k are a k -way partition of the original graph \mathcal{G} if $A_i \cap A_j = \emptyset$ for different i, j , and $\cup_{i=1}^k A_i = \mathcal{V}$. The objective of the k -way partitioning problem can be defined by

$$\rho(k) := \min_{A_1, \dots, A_k} \max_{1 \leq i \leq k} \Phi(A_i). \quad (12)$$

Following the definition of the objective, the partition tries to enforce that the conductance of any cluster A_i is at most the $\rho(k)$, i.e., the k -way expansion constant. Finding the optimal partition that optimizes the $\rho(k)$ is generally not computationally efficient for large-scale networks. Moreover, solving the k optimal cuts on a graph, such as to search for the optimal solution of (12) is usually NP-hard [17]. Nonetheless, the spectral clustering algorithm provides an approximation of the true optimum of the NP-hard problem. To be specific, Lee et al. [18] proved that performing spectral clustering on a graph G provides a bound for the k -way expansion constant, defined by higher order Cheeger inequality

$$\frac{\lambda_k}{2} \leq \rho(k) \leq O(k^2) \sqrt{\lambda_k}, \quad (13)$$

where $0 \leq \lambda_1 \leq \dots \leq \lambda_n \leq 2$ are the sorted eigenvalues of the normalized Laplacian matrix of the original graph and λ_1 is the smallest eigenvalue. Equation (13) suggests that a graph \mathcal{G} can have clusters with good quality if and only if the eigenvalue λ_k is small, which leads to a small k -way expansion constant. Whereas the practical approach for choosing the optimal K is not only determined by the Cheeger inequality, which always gives the best result when choosing K to be one. In general, Lee et al. [18] suggested to choose K as the number associated with a large eigengap. They show that if there is a significant gap between the eigenvalues of \mathcal{G} , then (13) can be rewritten to be independent on K

$$\max_{1 \leq i \leq k} \Phi(A_i) \leq \sqrt{\lambda_k / \delta^3} \quad (14)$$

where $\delta \in (0, \frac{1}{3})$, and λ_k is the k th smallest eigenvalue of the graph Laplacian L . That is, after obtaining the eigengap results from (11), we need to choose the K corresponding to a relatively large eigengap $\gamma_n(\lambda_k)$. This choice of K not only leads to a small graph expansion constant with a small eigenvalue, but also provides a reasonable number of dimensions for the spectral embedding.

E. Working With Renewables

All the Laplacian matrices defined in the previous sections are static and do not take the system's dynamic response into consideration. Moreover, the different behavior of the renewable generation is not covered. Thus, in this section, how to derive the dynamic response of the renewable generation coupled in the power grid is discussed. In [19], the authors have analyzed the major factor for deriving the dynamic response of the renewable generation. Take a wind power plant (WPP) as an example: if the WPP capacity is large, then the PCC transient response will be dominated by converter dynamics. In this case, the WPP will operate as a separate electrical area because of the distinct behavior different from nearby synchronous generators. However, if the WPP capacity is relatively low, then the WPP transient response at PCC is imposed by the rest of the power system and the WPP dynamic response is coherent with other generators. As a result, the PCC dynamics can be used as a proxy to identify the coherence of the renewable with other components inside the grid. Thus, this study adopts a measurement-based method and utilizes frequency deviation signals from system nominal frequency to identify generator coherency with the presence of renewable generations, and the coherency is treated as another type of Laplacian matrix for the generator dynamic information in the clustering algorithm.

The frequency deviation signal at each bus i can be obtained by

$$\Delta f_{i,t+\Delta t} = \frac{1}{\omega_0} \left(\frac{\phi_{i,t+\Delta t} - \phi_{i,t}}{\Delta t} \right) \quad (15)$$

where ω_0 is the system nominal frequency, and ϕ_i is the voltage phase angle at bus i . With the temporal frequency deviation signals, the frequency deviation vector of bus i can be constructed from frequency deviation measurement at different time instants

$$\Delta f_i = [\dots, \Delta f_{i,t-\Delta t}, \Delta f_{i,t}, \Delta f_{i,t+\Delta t}, \dots]^T. \quad (16)$$

Once the frequency deviation vector of each bus after the disruption is obtained, the coherency between each pair of buses can be measured by the coherency coefficient CC_{ij} , which is derived from the Cosine similarity of the corresponding frequency deviation vectors

$$CC_{ij} = \frac{\Delta f_i \Delta f_j^T}{\|\Delta f_i\| \|\Delta f_j\|}. \quad (17)$$

Since we can derive the CC_{ij} for each pair of buses, or nodes in the graph, another weight matrix W_{ij}^f carrying dynamic information for the power system graph can be defined as

follows:

$$W_{ij}^f = \begin{cases} CC_{ij} & \text{if } (i, j) \in \mathcal{E} \\ 0 & \text{otherwise.} \end{cases} \quad (18)$$

With all the aforementioned analysis, the overall road map for conducting intentional islanding for HESs with renewable penetrations can be summarized as follows.

- 1) Instead of finding the generator coherency first, use different information to define multilayer graph Laplacian matrices for clustering:
 - topology $w_{ij} = 1 \forall ij \in \mathcal{E}$, measures the pure connectivity;
 - admittance $w_{ij} = 1/\sqrt{R_{ij}^2 + X_{ij}^2} \forall ij \in \mathcal{E}$, measures the strength of connections (electrical distance);
 - average power flow $w_{ij} = (|P_{ij}| + |P_{ji}|)/2 \forall ij \in \mathcal{E}$, measures the importance of a line during operation;
 - frequency deviation $w_{ij} = CC_{ij} \forall ij \in \mathcal{E}$, measures the coherency of the buses, after a disruptive event.
- 2) Construct the normalized Laplacian matrices and perform eigendecomposition. Analyze the eigengaps to determine the best number of clusters K , for deriving the Grassmann manifold.
- 3) Use Grassmann manifold to derive a unified Laplacian based on the multilayer information:

$$L_{\text{uni}} = \sum_{i=1}^M L_i - \alpha \sum_{i=1}^M U_i U_i^T.$$

- 4) Conduct hierarchical clustering with connectivity constraints on the unified Laplacian.

III. RESULTS OF CASE STUDIES

To validate the proposed clustering-based intentional islanding strategy, the IEEE 9-bus test system is used as the case study. We have modified the original test networks by including additional renewable generations, such as wind farms, to show the applicability of the intentional islanding for transmission networks with renewables. The simulation of the system dynamic response after disruptions within a 20 s time window is conducted in the power system simulator for engineering software, and line outages are simulated to happen at 2 s. An idle time of 0.5 s is imposed right after the occurrence of disruptions to simulate required response time of the system in real life. Both the synchronized generators are modeled by GRNROU, IEEE1 for the automatic voltage regulator, and IIEESGO for the governor system. As for the wind farm, the generator/convertor, electrical controller, and plant level controller are simulated by REGCA1, REECA1, and REPCA1 model, respectively. The time step of the dynamic simulation is 0.0083 s.

A. IEEE 9-Bus Test Network

First, to demonstrate the major ideas and steps of the proposed intentional islanding strategy, we use the IEEE 9-bus system as the baseline model to illustrate the details of the main steps of the algorithm. Fig. 2 shows the original layout of the IEEE 9-bus test case. The line outage happens at the transmission line (7,5), in

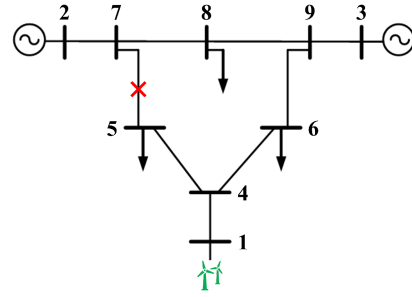


Fig. 2. One-line diagram of the IEEE 9-bus system, where the synchronous generator at bus 1 has been replaced by a wind farm (figure modified from [20]).

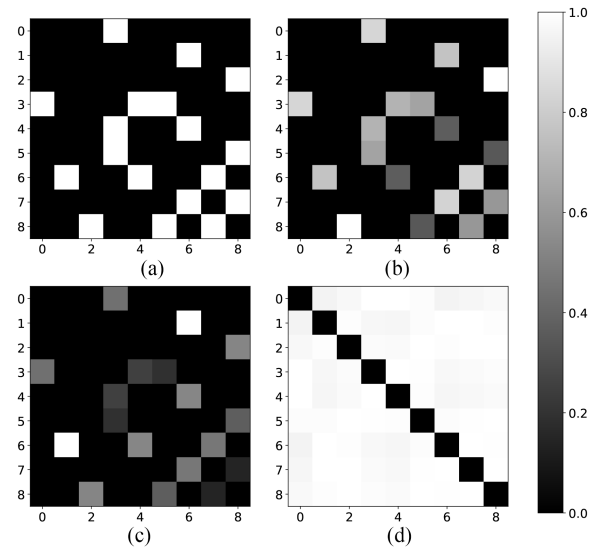


Fig. 3. Four weight matrices constructed from the measurement data of the IEEE 9-bus system. (a) Topology weight matrix W_{ij}^t . (b) Admittance weight matrix W_{ij}^a . (c) Power flow weight matrix W_{ij}^p . (d) Frequency deviation weight W_{ij}^f .

which the network has disconnected afterward. To incorporate the renewable generation, the synchronous generator at bus 1 has been replaced by a wind farm. The capacity of the wind power generation is set to be 100 MVA and consists of 30 wind turbines, and this renewable generation corresponds to 33.3% of the total power generation in the system. The original IEEE 9-bus system has a special characteristic that all three synchronous generators in the system have different operating modes, even before adding the renewable generation. Thus, this observation indicates that these three generators connecting at bus 1, 2, and 3 need to be partitioned into separate islands with an effective intentional islanding strategy after disruptions, and because of this characteristic, studies about intentional islanding algorithms usually use the 9-bus system as the baseline model.

As discussed in Section II-E, the first step for the clustering-based intentional islanding is to define the weight matrices for the system from different types of measurements. For the IEEE 9-bus system, four weight matrices are constructed, as shown in Fig. 3. From the matrices' data, it can be seen that except for the frequency deviation matrix, all other three matrices are

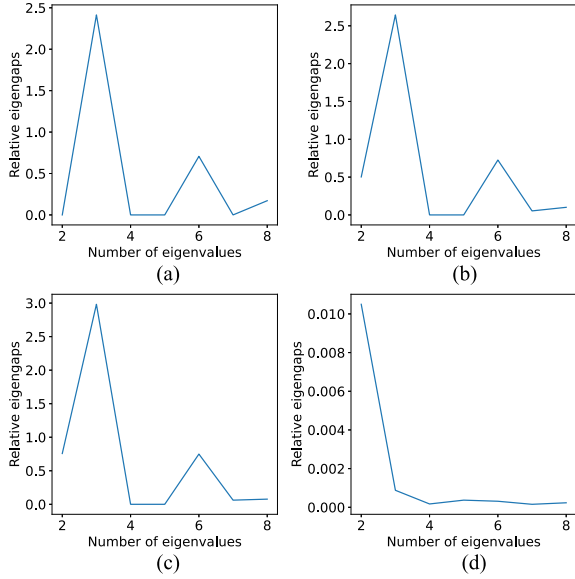


Fig. 4. Eigengap obtained from the four Laplacian matrices defined based on topology, admittance, power flow, and frequency deviation. (a) Eigengap of L_{ij}^t . (b) Eigengap of L_{ij}^a . (c) Eigengap of L_{ij}^p . (d) Eigengap of L_{ij}^f .

sparse and share the same structure. This is due to the nature of connectivity: the power flow and the admittance can only be nonzero if there is a line between two buses, and a power system is indeed a sparse graph, where the number of edges has the same scale as the number of nodes, i.e., $|\mathcal{E}| \propto |\mathcal{V}|$. In contrast, the frequency deviation matrix is obtained from the measurement of the dynamic system response, and the deviation is a pairwise relation between buses regardless of the connectivity of the system. Fig. 3 shows that the frequency deviation matrix W_{ij}^f has much more nonzero entries comparing to the topology, admittance, and power flow matrices. Thus, applying the Grassmann manifold to obtain a unified spectral embedding is a crucial task to conduct clustering because of the heterogeneous weight matrices.

Yet to derive the Grassmann manifold of the Laplacian matrices based on the weight matrices introduced previously, we first need to determine the number of dimensions K of the spectral embedding. As discussed in Section II-C, K is determined to be the number of i , which gives a large eigengap between two consecutive eigenvalues of the Laplacian matrix L . Thus, Fig. 4 shows the eigengap results of the Laplacian matrix of the IEEE 9-bus system. Notice that the X-axis starts from the second eigenvalue since the smallest eigenvalue of any valid Laplacian matrix is always zero. Hence, from the plot, K is chosen to be three in order to obtain the K -dimensional spectral embedding in the subspace for deriving the unified Laplacian matrix. Fig. 5 demonstrates the clustering result of the IEEE 9-bus system. After a disruption, the system operator can obtain an appropriate intentional islanding strategy based on the dendrogram. For example, if three islands are desired, then three clusters can be formed by cutting the tree at around 1.0 along the y-axis, and the corresponding three clusters are the subtrees that consist of buses $\{5, 1, 4\}$, $\{6, 3, 9\}$, and $\{8, 2, 7\}$.

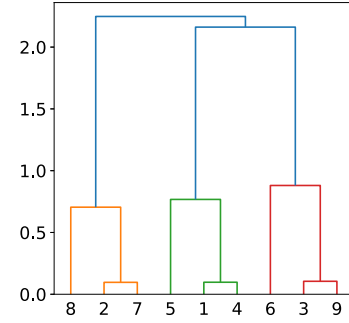


Fig. 5. Dendrogram result of the hierarchical clustering for IEEE 9-bus system.

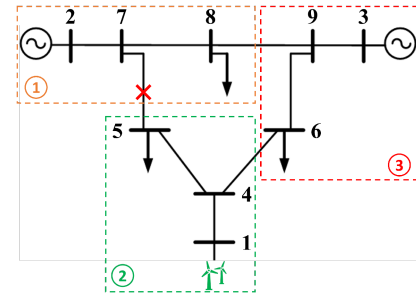


Fig. 6. Intentional islanding results for the IEEE 9-bus system based on the derived dendrogram (figure modified from [20]).

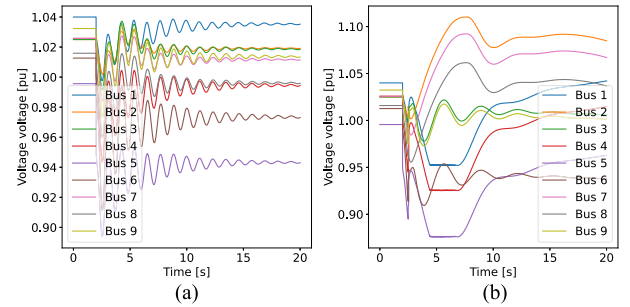


Fig. 7. Dynamic response of the voltage magnitude at all buses of the IEEE 9-bus system after disruptions, with and without the intentional islanding operation. (a) Without intentional islanding. (b) With intentional islanding.

Fig. 6 illustrates the IEEE 9-bus system after forming isolated islands following the results in the dendrogram. To analyze the system dynamic response after the disruption with and without intentional islanding strategy, Figs. 7 and 8 summarize the transient voltage magnitude and voltage angle measurements for the IEEE 9-bus test network, respectively. When the system undergoes a line outage without intentional islanding, Fig. 7 shows that the voltage magnitudes of all buses deteriorate from the nominal state to unstable cyclical patterns swinging between 0.92 and 1.04 pu. Although the voltage magnitudes have been self-stabilized toward the end of the simulation, the oscillations are so frequent that cascading failures maybe inevitable in practical applications. In comparison with the intentional islanding strategy, the voltage measurements of all buses swing around 0.9–1.1 pu with much smaller frequencies and have been

TABLE I
COMPARISON BETWEEN THE PROPOSED ISLANDING FRAMEWORK AND OTHER REFERENCES FOR IEEE 118-BUS SYSTEM

Reference	Method	Disruptive event	Number of islands	Total power deviations (MW)
[9]	Basic spectral clustering	Two line outages	2 (4)	384.2 (249.7)
[10]	Basic hierarchical clustering	Two line outages	6 (4)	327.3 (249.7)
[11]	Generator coherency identification	Two three-phase short circuits	2 (3)	169.0 (133.4)
[12]	Multi-source spectral clustering	Two line outages	3 (4)	239.4 (219.2)

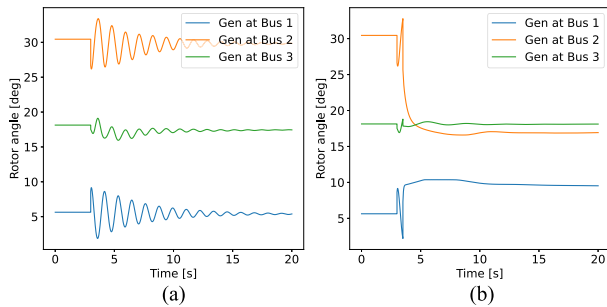


Fig. 8. Dynamic response of the rotor angle at all generators of the IEEE 9-bus system after disruptions, with and without the intentional islanding operation: notice the damped behavior after introducing the islanding action. (a) Without intentional islanding. (b) With intentional islanding.

stabilized at new steady states around 10 s. This difference is due to the fact that multiple lines, including the damaged line, are actively disconnected to enforce the system forming isolated subsystems, and each subsystem is powered by one generator solely to ensure that the operating conditions are consistent across the buses inside the same island.

Moreover, a more significant difference can be found by examining the dynamic rotor angle response of the machines. Fig. 8 suggests that the rotor angle of each generator becomes completely unstable while the angle of voltage would increase, and the system would be in the swing mode for a long period, which would consequently jeopardize the reliability and quality of the power if no intentional islanding is conducted. In contrast, with the help of the clustering action, the rotor angles stay within normal operating conditions, and the system can maintain nominal performance even with the presence of disruptions. This drastic difference in rotor angle response reveals the benefit of having the clustering-based intentional islanding as a contingency plan toward disruptions.

B. Comparative Analysis

The comparison results are derived from a larger scale IEEE 118-bus system, and four studies are considered as references, and to quantify the quality of the solutions, the power deviation after disruptions is used. The results for [11], [12] are obtained by running simulations following their original islanding solutions. But the underlying 118-bus system includes additional renewable generations. The numerical results are summarized in Table I. Numbers in parentheses represent results of our proposed method. Notice that all referenced studies are not considering renewable generations, which is one of the major focuses of this study, and methods proposed in [9], [10] are standard clustering algorithms without significant modifications for power

systems. This gap between the theoretical assumptions and practical applications leads to a large difference when comparing the performance of algorithms. On the other hand, neglecting renewables contributes to the difference in performance when comparing our method to that in [11], [12]. Especially for the generator coherency-based method: the coherency identification method has not been well studied for inverter-based technologies yet.

IV. CONCLUSION

To address the challenges of transmission system reliability along with the increasing level of renewable penetration, this study proposes a hierarchical clustering-based intentional islanding framework to guide the system transient operations after disruptions. Multiple layers of system real-time measurement data are considered including topology, electrical distance, as well as frequency deviation. To benefit from the heterogeneous information representing different aspects, this study adopts the Grassmann manifold algorithm to derive a unified embedding matrix for the final clustering. Moreover, because of the flexibility of the hierarchical clustering, the islanding decisions, i.e., the number of clusters formed, can be adjusted based on the stakeholders' prior knowledge. Also, to validate the proposed framework, the transient responses of the modified IEEE test feeder after disruptions have been studied. While emphasizing the fundamental islanding algorithm, we left few important aspects for future studies: incorporating distributed energy resources and considering islanding constraints to realize a practical islanding action. For example, for a power network with a high proportion of nuclear generations, the inertia monitoring and frequency response of each island when an imbalance between generation and load occurs can be included in future studies.

REFERENCES

- [1] N. Sharma, A. Tabandeh, and P. Gardoni, "Resilience analysis: A mathematical formulation to model resilience of engineering systems," *Sustain. Resilient Infrastructure*, vol. 3, no. 2, pp. 49–67, 2018.
- [2] M. Compare and E. Zio, "Predictive maintenance by risk sensitive particle filtering," *IEEE Trans. Rel.*, vol. 63, no. 1, pp. 134–143, Mar. 2014.
- [3] J. Wu and P. Wang, "Risk-averse optimization for resilience enhancement of complex engineering systems under uncertainties," *Rel. Eng. System Saf.*, vol. 215, 2021, Art. no. 107836. [Online]. Available: <https://www.sciencedirect.com/science/article/pii/S09511832021003562>
- [4] C. Chen, J. Wang, F. Qiu, and D. Zhao, "Resilient distribution system by microgrids formation after natural disasters," *IEEE Trans. Smart Grid*, vol. 7, no. 2, pp. 958–966, Mar. 2016.
- [5] J. Wu and P. Wang, "A comparison of control strategies for disruption management in engineering design for resilience," *ASCE-ASME J. Risk Uncertainty Eng. Syst., Part B: Mech. Eng.*, vol. 5, no. 2, Apr. 2019, Art. no. 020902, doi: [10.1155/2011/308245](https://doi.org/10.1155/2011/308245).

- [6] H. Wu, P. Dong, and M. Liu, "Distribution network reconfiguration for loss reduction and voltage stability with random fuzzy uncertainties of renewable energy generation and load," *IEEE Trans. Ind. Informat.*, vol. 16, no. 9, pp. 5655–5666, Sep. 2020.
- [7] A. Bidram, B. Poudel, L. Damodaran, R. Fierro, and J. M. Guerrero, "Resilient and cybersecure distributed control of inverter-based islanded microgrids," *IEEE Trans. Ind. Informat.*, vol. 16, no. 6, pp. 3881–3894, Jun. 2020.
- [8] J. Wu and P. Wang, "Post-disruption performance recovery to enhance resilience of interconnected network systems," *Sustain. Resilient Infrastructure*, vol. 6, no. 1–2, pp. 107–123, 2021.
- [9] A. Esmacilian and M. Kezunovic, "Prevention of power grid blackouts using intentional islanding scheme," *IEEE Trans. Ind. Appl.*, vol. 53, no. 1, pp. 622–629, Jan./Feb. 2017.
- [10] R. J. Sánchez-García et al., "Hierarchical spectral clustering of power grids," *IEEE Trans. Power Syst.*, vol. 29, no. 5, pp. 2229–2237, Sep. 2014.
- [11] E. Saadipour-Hanzaie, T. Amraee, and S. Kamali, "Minimal controlled islanding with similarity-based coherency identification using phasor measurement data," *IEEE Trans. Ind. Informat.*, vol. 18, no. 5, pp. 3256–3266, May 2022.
- [12] M. Dabbaghjamesh et al., "A novel two-stage multi-layer constrained spectral clustering strategy for intentional islanding of power grids," *IEEE Trans. Power Del.*, vol. 35, no. 2, pp. 560–570, Apr. 2020.
- [13] H. Sadeghi, M. Rashidinejad, and A. Abdollahi, "A comprehensive sequential review study through the generation expansion planning," *Renewable Sustain. Energy Rev.*, vol. 67, pp. 1369–1394, 2017. [Online]. Available: <https://www.sciencedirect.com/science/article/pii/S1364032116305378>
- [14] R. C. de Amorim, "Feature relevance in ward's hierarchical clustering using the l_p norm," *J. Classification*, vol. 32, no. 1, pp. 46–62, 2015.
- [15] X. Dong, P. Frossard, P. Vandergheynst, and N. Nefedov, "Clustering on multi-layer graphs via subspace analysis on Grassmann manifolds," *IEEE Trans. Signal Process.*, vol. 62, no. 4, pp. 905–918, Feb. 2014, doi: [10.1109/TSP.2013.2295553](https://doi.org/10.1109/TSP.2013.2295553).
- [16] R. Peng, H. Sun, and L. Zanetti, "Partitioning well-clustered graphs: Spectral clustering works!," *SIAM J. Comput.*, vol. 46, no. 2, pp. 710–743, 2017.
- [17] M. R. Garey, D. S. Johnson, and L. Stockmeyer, "Some simplified NP-complete graph problems," *Theor. Comput. Sci.*, vol. 1, no. 3, pp. 237–267, 1976.
- [18] J. R. Lee, S. Oveis Gharan, and L. Trevisan, "Multi-way spectral partitioning and higher-order Cheeger inequalities," in *Proc. Annu. ACM Symp. Theory Comput.*, 2012, pp. 1117–1130.
- [19] A. M. Khalil and R. Iravani, "Power system coherency identification under high depth of penetration of wind power," *IEEE Trans. Power Syst.*, vol. 33, no. 5, pp. 5401–5409, Sep. 2018.
- [20] Y. Song, D. J. Hill, and T. Liu, "Small-disturbance angle stability analysis of microgrids: A graph theory viewpoint," in *Proc. IEEE Conf. Control Appl.*, 2015, pp. 201–206.



Jiaxin Wu received the B.S. degree in mechanical engineering from the University of Wisconsin-Madison, Madison, WI, USA, in 2016, and the M.S. degree in mechanical engineering from the University of Illinois-Urbana Champaign, Champaign, IL, USA, in 2018, where he is currently working toward the Ph.D. degree in industrial and enterprise systems engineering.

His research interests include discrete optimization, system resilience analysis, and disruption management, with an emphasis on applications including renewable energy systems, supply chain systems as well as critical infrastructure networks.



Xin Chen received the B.S. degree in computational mathematics from Xiangtan University, Xiangtan, China, in 1995, M.S. degree in computational mathematics from the Chinese Academy of Sciences, Beijing, China, in 1998, and Ph.D. degree in operations research from MIT, Cambridge, MA, USA, in 2003.

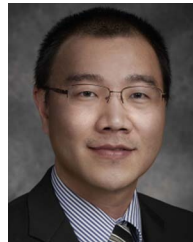
He is currently a Professor with the University of Illinois at Urbana-Champaign, Champaign, IL, USA. He has authored or coauthored the book *The Logic of Logistics: Theory, Algorithms, and Applications for Logistics and Supply Chain Management*. His research interests include optimization, data analytics, revenue management, and supply chain management.



Sobhan Badakhshan (Graduate Student Member, IEEE) received the B.S. degree in electrical engineering from the Iran University of Science and Technology, Tehran, Iran, in 2013, and the M.S. degree in electrical engineering from the Sharif University of Technology, Tehran, Iran, in 2015. He is currently working toward the Ph.D. degree in electrical engineering with the University of Texas-Dallas, Richardson, TX, USA.

His research interests include economic and secure optimization of electric power systems, energy system optimization, renewable energy integration, smart grids, future energy markets, generation scheduling, operation of integrated energy system, demand side management, and low-carbon power planning.

He is a Member of the Iran National Elites Foundation.



Jie Zhang (Senior Member, IEEE) received the B.S. and M.S. degrees in mechanical engineering from the Huazhong University of Science and Technology, Wuhan, China, in 2006 and 2008, respectively, and the Ph.D. degree in mechanical engineering from Rensselaer Polytechnic Institute, Troy, NY, USA, in 2012.

He is currently an Associate Professor with the Department of Mechanical Engineering and (Affiliated) Department of Electrical and Computer Engineering, University of Texas at Dallas, Richardson, TX, USA. His research interests include renewable energy grid integration, complex networks, big data analytics, energy management, and multidisciplinary design optimization.



Pingfeng Wang (Member, IEEE) received the doctoral degree in mechanical engineering from the University of Maryland, College Park, MD, USA, in 2010.

He is currently the Jerry S. Dobrovolsky Faculty Scholar and an Associate Professor with the Department of Industrial and Enterprise Systems Engineering, University of Illinois at Urbana-Champaign, Champaign, IL, USA, and an affiliate Associate Professor with Materials Research Laboratory at Illinois, University of Illinois at Urbana-Champaign. His research interests include engineering system design for reliability, failure resilience and sustainability, and prognostics and health management.

He is a Member of ASME and AIAA. He is the President of QCRE division at IISE.